VIP Solid-State Structures

DOI: 10.1002/anie.200905997

# Ferroelectricity in Perovskites with $s^0$ A-Site Cations: Toward Near-Room-Temperature Multiferroics**

*Erjun Kan, Hongjun Xiang, Changhoon Lee, Fang Wu, Jinlong Yang, and Myung-Hwan Whangbo**

Magnetic ferroelectric (FE) materials (that is, multiferroics) have received much attention and can have wide technological applications owing to the possibility of controlling their electric properties and their magnetic properties by electric fields.[1,2] An important class of multiferroic and FE[3] materials is based on perovskites, $ABO_3$, with two different cations A and B (for example $A^{2+}$ and $B^{4+}$ or $A^{3+}$ and $B^{3+}$), in which corner-sharing $BO_6$ octahedra form the three-dimensional lattice with every $B_8$ cube containing one A cation. An ideal cubic perovskite, in which the B-O–B bonds are linear with A located at the center of each $B_8$ cube (thus forming a $AO_{12}$ polyhedron), is expected when the tolerance factor $\tau = (r_O + r_A)/\sqrt{2}(r_O + r_B)$ is unity ($r_A$ and $r_B$ are the ionic radii of the A and B cations, respectively, with $r_O$ as that of the $O^{2-}$ anion). In most cases, the A cations are small, so that $\tau < 1$ and the A–O bonds are too long to maintain the ideal cubic structure. Consequently, the A cation moves away from the center of the $B_8$ cube, which is accompanied by the bending of the B-O-B bonds and the rotation of the $BO_6$ octahedra to form a lower-coordinate $AO_n$ polyhedron ($n < 12$) with short A–O bonds. The distortion of the ideal cubic perovskite toward a non-centrosymmetric FE structure requires another local instability apart from $\tau < 1$, namely, the second-order Jahn–Teller (SOJT) instability[4–6] of the A-site and/or B-site cation.

As found for $PbTiO_3$,[7] $PbVO_3$,[8] and $BiCoO_3$,[9] moving the A cation toward the center of one $B_4$ face (Figure 1a) leads to a tetragonal FE structure with space group *P*4*mm*. The B cations move away from the approaching A cations such that the coordinate environment of each B cation is more like a $BO_5$ square pyramid with shortened axial B–O bond. In $PbTiO_3$, $PbVO_3$, and $BiCoO_3$, the $s^2$ A-site cations $Pb^{2+}$ and $Bi^{3+}$ are susceptible to a SOJT distortion, which mixes the empty 6p orbital of A into the filled $6s^2$ orbital of A hence forming a lone pair on A.[4] In $PbTiO_3$, the B-site cation $Ti^{4+}$ ($d^0$) is also susceptible to a SOJT distortion, which mixes the empty Ti 3d orbitals into the filled 2p orbitals of the oxygen atom of the axial Ti–O bond.[5,6] Thus, in $PbTiO_3$, the need to make short Pb–O bonds and the SOJT instabilities of both $Pb^{2+}$ and $Ti^{4+}$ ions cooperate to give rise to the observed FE distortion.[10,11]

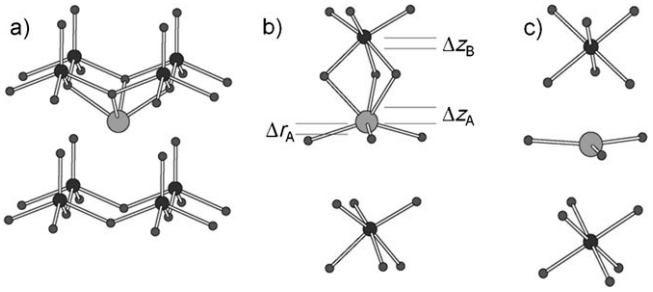


***Figure 1.*** Perspective views of the local structures around the A cation in three perovskites $ABO_3$, where the large, medium, and small circles refer to the A, B, and O atoms, respectively. a) The FE distortion in $ABO_3$ with space group *P*4*mm*. Only eight corner-sharing $BO_5$ square pyramids and one A cation are shown. b) The FE distortion of $ABO_3$ with space group *R*3*c*. For simplicity, only the two $BO_6$ octahedra at the two corners of the $B_8$ cube along the body-diagonal direction and the $AO_3$ unit lying between the two octahedra are shown. The $AO_3$ unit merges with the upper $BO_6$ octahedron to form a distorted $AO_6$ octahedron, which shares its face with the upper $BO_6$ octahedron, resulting in the face-sharing octahedral dimer $ABO_9$. c) The PE structure of $ABO_3$ with space group $R\bar{3}c$, by which one FE structure is converted into the other FE structure with opposite polarization. The B cation in each $BO_6$ octahedron is located at the center of the $O_6$ octahedron, and the $AO_3$ unit lying at the midpoint between the two octahedra is planar.

Another type of the A-cation displacement from the center of the $B_8$ cube is the movement toward one corner of the $B_8$ cube along the body-diagonal direction (that is, the $C_3$ rotational axis; Figure 1b) to form a non-centrosymmetric FE trigonal structure with space group *R*3*c*, as found for $BiFeO_3$.[12] The movement of the A cation toward one corner is equivalent to that toward the opposite corner, and the two energetically-equivalent FE structures are mutually interconverted through the centrosymmetric paraelectric (PE) trigonal structure with space group $R\bar{3}c$ (Figure 1c).[13,14] For $BiFeO_3$, the FE Curie temperature ($T_E = 1123$ K)[15] and the three-dimensional antiferromagnetic ordering temperature ($T_N = 650$ K)[16] are well above room temperature. For

[*] Dr. E. Kan, Dr. C. Lee, Prof. M.-H. Whangbo
Department of Chemistry, North Carolina State University
Raleigh, NC 27695-8204 (USA)
E-mail: mike_whangbo@ncsu.edu
Dr. H. Xiang
National Renewable Energy Laboratory, Golden (USA)
Dr. F. Wu
School of Science, Nanjing Forestry University (P. R. China)
Prof. J. Yang
Hefei National Laboratory for Physical Sciences at Microscale
University of Science and Technology of China (P. R. China)

[**] The work at NCSU was supported by U.S. DOE under Grant No. DE-FG02-86ER45259 and by the resources of the NERSC Center. The work in China was supported by National Natural Science Foundation of China (50121202, 20533030, 10474087), National Key Basic Research Program under Grant No.2006CB922004, the USTC-HP HPC project, and the SCCAS and Shanghai Supercomputer Center.

practical applications, it is highly desirable to find multiferroics with both $T_E$ and $T_N$ close to room temperature. Recently, Belik et al.[17] have achieved a partial success toward this goal; they synthesized the indium-based multiferroics $(In_{1-x}M_x)MO_3$ ($x \approx 0.112$-$0.176$; $M = Mn_{0.5}Fe_{0.5}$) that have a $T_N$ value close to room temperature; however, $T_E$ is still high (for $x = 0.176$, $T_N \approx 270$ K and $T_E$ is expected to be above 670 K, but the phase is transformed irreversibly to a corundum-type structure above 670 K). These multiferroics, which are isostructural with $BiFeO_3$, are quite surprising in two aspects. First, magnetic ordering of a system made up of magnetic ions is generally prevented when disorder is present in the system. However, long-range magnetic ordering occurs near room temperature despite the expected disorder in the A and B sites (that is, the statistical distribution of high-spin $Mn^{3+}$ and $Fe^{3+}$ cations). Second, it is believed that the strong FE distortion in perovskites with $s^2$ A-site cations, such as $BiFeO_3$, $PbTiO_3$, $PbVO_3$, and $BiCoO_3$, arises from the need to create space for the lone pair on A. However, a strong FE distortion that is almost as strong as found for $BiFeO_3$ occurs in the indium-based multiferroics, although the A-site cations ($In^{3+}$, $Mn^{3+}$, and $Fe^{3+}$) do not possess a lone pair. Herein, we explore these puzzling observations on the basis of systematic density functional calculations for $BiFeO_3$ and model perovskites $ABO_3$ (A = Ga, In, Tl; B = Mn, Fe, $Mn_{0.5}Fe_{0.5}$) that simulate the indium-based multiferroics $(In_{1-x}M_x)MO_3$.

Unless stated otherwise, our calculations were carried out for the antiferromagnetic (AFM) states of $ABO_3$ (A = Ga, In, Tl; B = Mn, Fe, $Mn_{0.5}Fe_{0.5}$) and $BiFeO_3$ in which all nearest-neighbor (NN) spins of the B-site cations are antiferromagnetically coupled. In the hexagonal setting of the trigonal space group *R*3*c*, a unit cell of these compounds has six layers of B cations perpendicular to the *c* axis. To simulate the random arrangement of the $Mn^{3+}$ and $Fe^{3+}$ ions in $A(Mn_{0.5}Fe_{0.5})O_3$, we adopted the ordered arrangement in which layers of $Mn^{3+}$ ions alternate with layers of $Fe^{3+}$ ions along the *c* direction. This arrangement is statistically most probable because each $B_8$ cube is given by $Mn_4Fe_4$ such that all NN cations are different. In our GGA + U calculations for the FE structures of $ABO_3$ (A = Ga, In, Tl; B = Mn, Fe, $Mn_{0.5}Fe_{0.5}$) and $BiFeO_3$ (with space group *R*3*c*), the positions of the atoms were fully optimized but the cell parameters were kept constant at the experimental values. The cell parameters of $ABO_3$ (A = Ga, In, Tl; B = Mn, Fe, $Mn_{0.5}Fe_{0.5}$) were fixed at those found for $(In_{1-x}M_x)MO_3$ ($x \approx 0.176$; M = $Mn_{0.5}Fe_{0.5}$).[17]

The results of our structure optimizations for the FE structures of $ABO_3$ are summarized in terms of the three parameters $\Delta r_A$, $\Delta z_A$ and $\Delta z_B$ (Figure 1b), where $\Delta r_A$ is the A-cation displacement from the center of the $B_8$ cube to the actual position of A in the $B_8$ cube; the strength of the $AO_6$ ($BO_6$) octahedron distortion is measured by the displacement $\Delta z_A$ ($\Delta z_B$) from the center of the $O_6$ octahedron to the actual position of the A (B) cation. Given that the *z* axis taken along the *c* direction of the hexagonal setting (i.e., the body-diagonal direction of the $B_8$ cube; Figure 1b) shows that $\Delta z_A < 0$ and $\Delta z_B > 0$. The values of $\Delta r_A$ are summarized in Table 1, and the $\Delta z_A$ and $\Delta z_B$ values are given in Table 2. The $\Delta r_A$ values are substantial, and are largely determined by the A cation. For a given $ABO_3$ series and $BiFeO_3$, the $\Delta r_A$ values decrease in the order $Ga^{3+} > In^{3+} > Tl^{3+} > Bi^{3+}$, which reflects that the A-cation size increases in the order $Ga^{3+} < In^{3+} < Tl^{3+} < Bi^{3+}$. Table 2 reveals that the $\Delta z_A$ and $\Delta z_B$ values are substantial and are largely determined by the A cation; the $|\Delta z_A|$ values increase in the order $Ga^{3+} < In^{3+} < Tl^{3+}$, and the $\Delta z_B$ values decrease with increasing $|\Delta z_A|$. The $\Delta z_A$ and $\Delta z_B$ values of $BiFeO_3$ are close to those of $TlFeO_3$.

***Table 1:*** Values of $\Delta r_A$ calculated for $ABO_3$.[a]

| A | $A(Mn_{0.5}Fe_{0.5})O_3$ | $AMnO_3$ | $AFeO_3$ |
|---|---|---|---|
| Ga | 0.588 | 0.550 | 0.593 |
| In | 0.504 | 0.479 | 0.559 |
| Tl | 0.321 | 0.309 | 0.339 |

[a] B = $Mn_{0.5}Fe_{0.5}$, Mn, Fe. $\Delta r_A = 0.295$ Å for $BiFeO_3$.

***Table 2:*** Values of $\Delta z_A$ and $\Delta z_B$ calculated for $ABO_3$.[a]

| B | Parameter | $GaBO_3$ | $InBO_3$ | $TlBO_3$ |
|---|---|---|---|---|
| $Mn_{0.5}Fe_{0.5}$ | $\Delta z_B$(Mn) | 0.235 | 0.185 | 0.108 |
| | $\Delta r_A$(Mn) | −0.360 | −0.479 | −0.747 |
| | $\Delta z_B$(Fe) | 0.282 | 0.234 | 0.137 |
| | $\Delta r_A$(Fe) | −0.318 | −0.449 | −0.720 |
| Mn | $\Delta z_B$ | 0.226 | 0.182 | 0.136 |
| | $\Delta r_A$ | −0.345 | −0.467 | −0.745 |
| Fe | $\Delta z_B$ | 0.269 | 0.216 | 0.122 |
| | $\Delta r_A$ | −0.344 | −0.468 | −0.732 |

[a] A = Ga, In, Tl; B = $Mn_{0.5}Fe_{0.5}$, Mn, Fe. $\Delta z_A = -0.641$ Å and $\Delta z_B = 0.193$ Å for $BiFeO_3$.

As described above, the FE distortion of the indium-based multiferroics $(In_{1-x}M_x)MO_3$ ($x \approx 0.112$–$0.176$; $M = Mn_{0.5}Fe_{0.5}$) is very similar in nature and magnitude to that found in $BiFeO_3$, which suggests that the origin of their FE distortions is identical. The face-sharing octahedral dimer $ABO_9$ (Figure 1b) along the body-diagonal direction of the $B_8$ cube can be regarded as a result of the interaction between the $BO_6$ octahedron and the $AO_3$ pyramid (Figure 2a). As depicted in Figure 2b, the $AO_3$ pyramid has two hydrid orbitals $\phi_+$ and $\phi_-$ made up of the ns and np orbitals ($n = 4$, 5, 6 for $Ga^{3+}$, $In^{3+}$, and $Tl^{3+}$, respectively).[4] In the case of the $s^2$ cation $Bi^{3+}$, the $\phi_+$ orbital is doubly occupied to become a lone pair, whilst the $\phi_-$ orbital is empty. In the case of the $s^0$ cations $Ga^{3+}$, $In^{3+}$ and

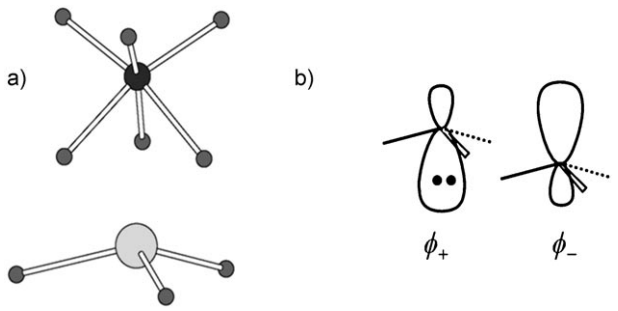


***Figure 2.*** a) The face-sharing octahedral dimer $ABO_9$ in the FE structure of $ABO_3$ with space group *R*3*c* in terms of the $BO_6$ octahedron and the $AO_3$ pyramid. b) The two hybrid orbitals $\phi_+$ and $\phi_-$ of the $AO_3$ pyramid.

  

$Tl^{3+}$, both $\phi_+$ and $\phi_-$ orbitals are empty. The energy lowering associated with the interaction of the $AO_3$ pyramid with the $BO_6$ octahedron occurs primarily from the interaction of the empty $\phi_-$ orbital with the filled 2p orbitals of the three oxygen atoms that form the A–O bonds. This interaction is the driving force for the SOJT distortion of the A-site cations, and is therefore independent of whether the A-site cation is an $s^0$ or an $s^2$ cation. It was shown above that the $|\Delta z_A|$ values increase in the order $Ga^{3+} < In^{3+} < Tl^{3+}$, whereas the $\Delta z_B$ values decrease with increasing $|\Delta z_A|$. The extent of the $A^{3+}$ cation displacement in the $AO_6$ octahedron from the center of the $O_6$ octahedron is related to the extension of the $A^{3+}$-cation np orbital ($n = 4$, 5, and 6 for $Ga^{3+}$, $In^{3+}$, and $Tl^{3+}$, respectively); the maximum overlap of the $A^{3+}$ cation $\phi_-$ orbital (hence the np orbital) with the O 2p orbitals of the three oxygen atoms forming the A–O bonds should occur at a larger $|\Delta z_A|$ value as the A cation is varied from $Ga^{3+}$ to $In^{3+}$ to $Tl^{3+}$. The involvement of the $In^{3+}$ cation 5p orbitals in the FE distortion of the perovskite $InBO_3$ (B = Mn, Fe, $Mn_{0.5}Fen_{0.5}$) can be seen from the plots of the density of states (DOS) calculated for the FE and PE structures of $InFeO_3$ (Figure 3). The PE structure has more unoccupied

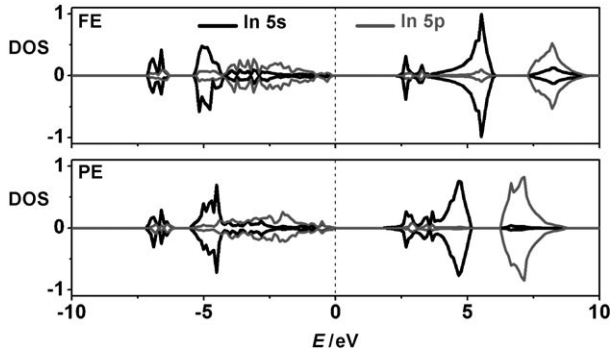


***Figure 3.*** Plots of the projected DOS (states/eV per two formula units) calculated for the In 5s and In 5p orbitals in the FE and PE structures of $InFeO_3$. The up- and down-spin densities are indicated by plus and minus DOS values, respectively.

In 5p states in a lower energy region than does the FE structure. This result means that more In 5p states are involved in bonding with the O 2p states in the FE state than in the PE state, as expected from the SOJT distortion involving the $In^{3+}$ cation. Similar interactions should occur between the np orbitals of the A-site cation and the O 2p orbitals in the FE structure of $ABO_3$ with space group *P4mm*, as found for $PbVO_3$.[18]

We then examined the FE polarization of $(In_{1-x}M_x)MO_3$ ($x \approx 0.176$; $M = Mn_{0.5}Fe_{0.5}$) by considering only the perovskites $AFeO_3$ (A = Ga, In, Tl), because the FE distortion is largely determined by the A cation, as discussed above. As found for $BiFeO_3$,[13,14] the most probable PE structure of $AFeO_3$ (A = Ga, In, Tl) has the centrosymmetric structure with space group $R\bar{3}c$.[19] The rhombohedral setting of this structure has the positions Fe(0,0,0), In($^1/_4$,$^1/_4$,$^1/_4$), and O($x$,$^1/_2-x$,$^1/_4$). Our structure optimizations for the PE structures lead to $x = 0.6023$, 0.6399, 0.6405, and 0.6707 for $GaFeO_3$, $InFeO_3$, $TlFeO_3$, and $BiFeO_3$, respectively. Given the FE and PE structures of $AFeO_3$, we calculated their FE polarizations $P$ (along the body-diagonal direction of the $B_8$ cube) on the basis of the Berry phase method,[20] which leads to 46, 74, and 139 $\mu C\,cm^{-2}$ for $GaFeO_3$, $InFeO_3$, and $TlFeO_3$, respectively. These values are comparable to 98.7 $\mu C\,cm^{-2}$ calculated for $BiFeO_3$.[13,14] Experimentally, the FE polarization of $(In_{1-x}M_x)MO_3$[17] is comparable in magnitude to that of $BiFeO_3$[13,14] ($P \approx 1\ \mu C\,cm^{-2}$ for $x = 0.143$ versus 2–6 $\mu C\,cm^{-2}$).

To understand why $(In_{1-x}M_x)MO_3$ ($M = Mn_{0.5}Fe_{0.5}$) has a significantly lower $T_N$ (about 270 K for $x \approx 0.176$) than does $BiFeO_3$ (650 K), it is necessary to evaluate the NN spin exchange parameters $J$ of $InMO_3$ (M = Mn, Fe, $Mn_{0.5}Fe_{0.5}$) and $BiFeO_3$ by calculating the energies of the two ordered spin states for $InMO_3$ and $BiFeO_3$; that is, the AFM state considered so far and the ferromagnetic (FM) state in which all NN spins are ferromagnetically coupled. By mapping the energy difference between the two states onto the corresponding energy difference expected from the spin Hamiltonian expressed in terms of $J$,[21,22] we obtain $J = -18.8$, $-14.6$, $+10.4$, and $-6.1$ meV for $BiFeO_3$, $InFeO_3$, $InMnO_3$, and $In(Mn_{0.5}Fe_{0.5})O_3$, respectively. Namely, the AFM state is more stable than the FM state for $InFeO_3$ and $In(Mn_{0.5}Fe_{0.5})O_3$, as found for $BiFeO_3$, whereas the opposite is the case for $InMnO_3$.[23,24] Note that the $J$ value of $In(Mn_{0.5}Fe_{0.5})O_3$ is smaller than those of $InFeO_3$ and $BiFeO_3$ by a factor of about 2.5–3. In the mean field approximation,[25] $T_N$ scales linearly with $|J|$, so that the $T_N$ of $In(Mn_{0.5}Fe_{0.5})O_3$ is estimated to be circa 220–260 K from $T_N = 650$ K for $BiFeO_3$. The latter value is quite close to that found for the indium-based multiferroics $(In_{1-x}M_x)MO_3$ ($M = Mn_{0.5}Fe_{0.5}$) (i.e., about 270 K for $x \approx 0.176$).[17] Therefore, the three-dimensional magnetic ordering of $(In_{1-x}M_x)MO_3$ ($M = Mn_{0.5}Fe_{0.5}$) near room temperature arises from two factors: one is that the statistically most probable distribution of the $Mn^{3+}$ and $Fe^{3+}$ ions in the $b$ sites leads to the three-dimensional arrangement in which the spin exchange paths between these magnetic ions are largely given by the Mn-O-Fe superexchanges; the other factor is that the Mn-O-Fe superexchange is weaker than the Fe-O-Fe superexchange by a factor of about three.

Finally, we addressed the question of how to lower $T_E$ of perovskite multiferroics with $s^0$ A-site cations by considering $AFeO_3$ (A = Ga, In, Tl, Bi). It is not surprising that the indium-based multiferroics $(In_{1-x}M_x)MO_3$ ($M = Mn_{0.5}Fe_{0.5}$) have a high $T_E$ and a high FE polarization because their FE distortion is nearly as strong as that found for $BiFeO_3$. Qualitatively, $T_E$ of $AFeO_3$ (A = Ga, In, Tl, Bi) is expected to be lowered when the stability of the FE structure with respect to the PE structure is reduced. Our calculations for the optimized FE and PE structures of $AFeO_3$ predict that the FE structure is more stable than the PE structure by 0.31, 0.45, 0.20, and 0.32 eV per formula unit for A = Ga, In, Tl, and Bi, respectively, suggesting that the tendency for the A-site cation to undergo an FE distortion should decrease in the order $In^{3+} > Bi^{3+}$, $Ga^{3+} > Tl^{3+}$. Therefore, $TlFeO_3$ would have a lower $T_E$ value than does $BiFeO_3$. It would be of interest to prepare the thallium analogue of the indium-based multi-

  

ferroics, such as $(Tl_{1-x}M_x)MO_3$ ($M = Mn_{0.5}Fe_{0.5}$). Another interesting compound would be $(Ga_{1-x}M_x)MO_3$ ($M = Mn_{0.5}Fe_{0.5}$), because the presence of $Mn^{3+}$ and $Fe^{3+}$ ions at the A-cation sites would reduce the tendency for the $Ga^{3+}$ ions to undergo an FE distortion, thus lowering $T_E$.

In summary, our work explains why $T_N$ of the indium-based multiferroic perovskites $(In_{1-x}M_x)MO_3$ ($M = Mn_{0.5}Fe_{0.5}$) is near room temperature and why the perovskites with $s^0$ and $s^2$ A-site cations have similar ferroelectric distortions. Possible perovskites with $T_E$ lower than that of $(In_{1-x}M_x)MO_3$ are expected from $(Tl_{1-x}M_x)MO_3$ ($M = Mn_{0.5}Fe_{0.5}$) and $(Ga_{1-x}M_x)MO_3$ ($M = Mn_{0.5}Fe_{0.5}$).

## Experimental Section

The calculations employed the projector-augmented wave method[26] encoded in the Vienna ab initio simulation package,[27] the PW91 functional form[28] of the generalized gradient approximation (GGA), and the plane-wave cut-off energy of 400 eV. The GGA plus on-site repulsion $U$ method[29] (GGA + $U$) was used to properly describe the electron correlation associated with the Mn and Fe 3d states with several values of $U$ for both manganese and iron. Similar results are obtained from the use of other $U$ values, so we report only those from $U = 4.5$ eV.

Received: October 24, 2009
Revised: December 17, 2009
Published online: February 1, 2010

**Keywords:** density functional calculations · ferroelectric distortion · indium · Jahn–Teller distortion · perovskite phases

[1] a) C. Ederer, N. A. Spaldin, *Curr. Opin. Solid State Mater. Sci.* **2005**, *9*, 128; b) R. Ramesh, N. A. Spaldin, *Nat. Mater.* **2007**, *6*, 21; c) D. Khomskii, *Physics* **2009**, *2*, 20.
[2] a) W. Eerenstein, N. D. Mathur, J. F. Scott, *Nature* **2006**, *442*, 759; b) S. W. Cheong, M. Mostovoy, *Nat. Mater.* **2007**, *6*, 13; c) Y. Tokura, *J. Magn. Magn. Mater.* **2007**, *310*, 1145.
[3] a) J. F. Scott, *Science* **2007**, *315*, 954; b) S. Leach, R. E. Garcia, *Mater. Sci. Forum* **2009**, *606*, 119.
[4] T. A. Albright, J. K. Burdett, M. H. Whangbo, *Orbital Interactions in Chemistry*, Wiley, New York, **1985**.
[5] M. H. Whangbo in *Crystal Chemistry and Properties of Materials with Quasi-One-Dimensional Structures* (Ed.: J. Rouxel), D. Reidel, Boston, **1986**, pp. 58–61.
[6] R. A. Wheeler, M. H. Whangbo, T. Hughbanks, R. Hoffmann, J. K. Burdett, T. A. Albright, *J. Am. Chem. Soc.* **1986**, *108*, 2222.
[7] A. Sani, M. Hanfland, D. Levy, *J. Solid State Chem.* **2002**, *167*, 446.
[8] A. A. Belik, M. Azuma, T. Saito, Y. Shimakawa, M. Takano, *Chem. Mater.* **2005**, *17*, 269.
[9] A. A. Belik, S. Iikubo, K. Kodama, N. Igawa, S. Shamoto, S. Niitaka, M. Azuma, Y. Shimakawa, M. Takano, F. Izumi, E. Takayama-Muromachi, *Chem. Mater.* **2006**, *18*, 798.
[10] As found for $BaTiO_3$.[11] The ideal cubic structure is also unstable when $\tau > 1$. In this case, the $Ti^{4+}$ ion ($d^0$) in each $TiO_6$ octahedron moves toward one oxygen atom to form a $TiO_5$ square pyramid owing to the SOJT instability of the $Ti^{4+}$ ion. In the FE structure of $BaTiO_3$, all $Ti^{4+}$ ions are displaced in one direction.
[11] D. J. Singh, C. H. Park, *Phys. Rev. Lett.* **2008**, *100*, 087601.
[12] A. Palewicz, R. Przenioslo, I. Sosnowska, A. Hewat, *Acta Crystallogr. Sect. B* **2007**, *63*, 537.
[13] J. B. Neaton, C. Ederer, U. Waghmare, N. A. Spaldin, K. M. Rabe, *Phys. Rev. B* **2005**, 71, 014113. This work assumed that the paraelectric phase has the $R\bar{3}c$ structure. Under high temperatures or high pressures, $BiFeO_3$ is known to have the *Pnma* phase.[14] However, there is no evidence that this *Pnma* phase is the paraelectric phase of $BiFeO_3$.
[14] G. Catalan, J. F. Scott, *Adv. Mater.* **2009**, *21*, 2463.
[15] J. R. Teague, R. Gerson, W. James, *Solid State Commun.* **1970**, *8*, 1073.
[16] S. Kiselev, G. Zhdanov, R. Ozerov, *Dokl. Akad. Nauk SSSR* **1962**, 145,1255.
[17] A. A. Belik, T. Furubayashi, Y. Matsushita, M. Tanaka, S. Hishita, E. Takayama-Muromachi, *Angew. Chem.* **2009**, *121*, 6233; *Angew. Chem. Int. Ed.* **2009**, *48*, 6117.
[18] D. J. Singh, *Phys. Rev. B* **2006**, *73*, 094102.
[19] Our calculations show that the energy of the corundum-type structure is too high compared with the ferroelectric structure by about 3 eV, and thus cannot be the paraelectric phase. In contrast, the centrosymmetric perovskite-type ($R\bar{3}c$) structure gives a very reasonable energy difference, and is therefore adopted in our analysis.
[20] a) R. King-Smith, D. Vanderbilt, *Phys. Rev. B* **1993**, *47*, 1651; b) R. Resta, *Rev. Mod. Phys.* **1994**, *66*, 899.
[21] The energy difference between the AFM and FM states, $\Delta E = E(\mathrm{AFM}) - E(\mathrm{FM})$, is calculated to be −235, −184, +83, and −61 meV per formula unit for $BiFeO_3$, $InFeO_3$, $InMnO_3$ and $In(Mn_{0.5}Fe_{0.5})O_3$, respectively. In terms of the spin Hamiltonian,[24] the corresponding energy difference is given by $\Delta E = 2J(N^2/4)$ for $BiFeO_3$ and $InFeO_3$, $\Delta E = 2J(M^2/4)$ for $InMnO_3$, and $\Delta E = 2J(MN/4)$ for $In(Mn_{0.5}Fe_{0.5})O_3$, where $M = 4$ and $N = 5$ are the number of unpaired spins at the high-spin $Mn^{3+}$ and $Fe^{3+}$ sites, respectively.
[22] a) D. Dai, M. H. Whangbo, *J. Chem. Phys.* **2001**, *114*, 2887; b) D. Dai, M. H. Whangbo, *J. Chem. Phys.* **2003**, *118*, 29.
[23] The perovskite structure adopted for $InMnO_3$ is a hypothetical one. Thus, this finding cannot be compared with the reported AFM coupling in $InMnO_3$ that does not have the perovskite structure ($P\bar{6}cm$).[24]
[24] A. A. Belik, S. Kamba, M. Savinov, D. Nuzhnyy, M. Tachibana, E. Takayama-Muromachi, V. Goian, *Phys. Rev. B* **2009**, *79*, 054411.
[25] J. Smart, *Effective Field Theory of Magnetism*, Saunders, Philadelphia, **1966**.
[26] P. Blöchl, *Phys. Rev. B* **1994**, *50*, 17953.
[27] a) G. Kresse, J. Hafner, *Phys. Rev. B* **1994**, *49*, 14251; b) G. Kresse, J. Furthmüller, *Comput. Mater. Sci.* **1996**, *6*, 15.
[28] J. P. Perdew, J. Chevary, S. Vosko, K. Jackson, M. Pederson, D. J. Singh, C. Fiolhais, *Phys. Rev. B* **1992**, *46*, 6671.
[29] S. Dudarev, G. Botton, S. Savrasov, C. Humphreys, A. Sutton, *Phys. Rev. B* **1998**, *57*, 1505.

  